Exploring the Relationship between Thyroid Hormones and Iodine Detection through X-ray Fluorescence Analysis in Biological Samples

A. Drake McFayden

May 2023

Abstract

Iodine concentration in raw thyroid glands is an important reporter on thyroid hormones and their function. First, iodine concentrations were detected through X-ray fluorescence (XRF) analysis. The thyroid glands were then processed into a fine powder and tested through high-performance liquid chromatography (HPLC) for correlation with triiodothyronine (T3) and thyroxine (T4) thyroid hormone concentrations. The results from 62 processed batches (31 raw lots) using the weighted average of the iodine concentrations from each input lot were then compared to the thyroid hormone concentration for each batch showing a moderate correlation. This information helps identify which lots are more likely to yield high potency material and improves process forecasting.

Table of Contents

Introduction

The primary role of iodine in vertebrate biology is to serve as a component of the thyroid hormones [1]. Iodine in raw thyroid samples can be detected by XRF analysis and thyroid hormones in processed thyroids can be detected by HPLC. A significant portion of iodine in the thyroid gland is in T3 and T4 hormones. By measuring iodine in raw thyroid samples, we should be able to correlate with the T3 and T4 concentrations in the samples. If correlation exists, it would be possible to monitor raw materials and identify trends several months before processing which could help forecasting for operations, sales, and procurement.

Our research goal is to establish the relationship between iodine concentration in raw thyroid glands and thyroid hormone concentration in fine milled thyroid powder?

Theory

X-Ray Fluorescence Analysis

Electrons are fixed at specific energies in their positions in an atom, and this determines their orbits. Additionally, the spacing between the orbital shells of an atom is unique to the atoms of each element, so an atom of iodine (I) has different spacing between its electron shells than an atom of sodium (Na), or potassium (K), etc.

When an X-ray source is aimed at a sample, the X-rays are absorbed by the electrons orbiting the nucleus in the atoms of the sample. If the energy absorbed is high enough, then the electron receiving the X-ray is released from the atom, leaving behind a vacancy, and making the atom unstable. The atom must immediately correct the instability by filling the vacancies with electrons from a farther away shell. When this occurs, a new X-ray is emitted as an X-ray fluorescence (XRF) photon which is unique for each element [2] providing an X-ray spectral signature or atomic fingerprint.

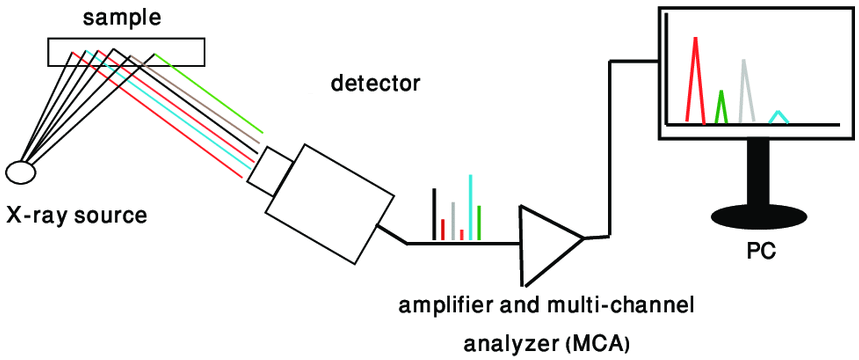

Figure 1 Schematic of ED-XRF.

These XRF photons can be detected with an XRF analyzer which contains two main components: an X-ray source to initiate XRF in the sample and a detector to determine the elements and their quantities within the sample. The X-ray source in the analyzer uses Bremsstrahlung radiation on an anode (tungsten in this experiment) to produce X-rays. Bremsstrahlung radiation occurs when high-energy electrons bombard the anode and as they penetrate into the target, some electrons travel close to the nucleus due to the attraction of its positive charge and are subsequently influenced by its electric field. The course of these electrons would be deflected, and a portion or all of their kinetic energy (KE) would be lost. The principle of the conservation of energy states that in producing the X-ray photon, the electron has lost some of its KE:

$$KE_{final} = KE_{initial} - E_{X-ray}$$

The "lost" energy is emitted as X-ray photons, specifically Bremsstrahlung radiation. The energy can range from zero to the maximum KE of the bombarding electrons (i.e., 0 to E_{max}, depending on how much the electrons are influenced by the electric field, therefore forming a continuous spectrum. The peak of the filtered spectrum typically occurs at approximately one-third of E_{max}. The unfiltered Bremsstrahlung spectrum demonstrates a ramp shape with the probability of

photon production being inversely linear with KE. In the XRF analysis conducted, the excitation source used has a variable energy range of 8 to 50 keV. [3]

The intensity of Bremsstrahlung radiation is proportional to the square of the atomic number of the target (Z), the number of unit charges of the bombarding particle (z) and inversely with the mass of the bombarding particle (m) [4]:

$$I \propto \frac{Z^2 z}{m}$$

The XRF analyzer's power, sensitivity, and ability to resolve the data are key factors to correctly identifying the quantities and types of atoms detected.

The energies of x-ray emissions lines for iodine are as follows: $K\alpha_1 = 24.6keV$, $K\alpha_2 = 28.3keV$, $K\beta_1 = 32.3\ keV$, $L\alpha_1 = 3.9keV$, $L\alpha_2 = 3.9keV$, $L\beta_1 = 4.2keV$, $L\beta_2 = 4.5keV$, $L\gamma_1 = 4.8keV$ [5].

To determine quantities, the spectrometers are calibrated to a standard with known concentrations of a material and are measured with intensity vs. concentration where a regression curve is fitted and the intensity of the detected sample is compared to the calibration curve of the standard.

High Performance Liquid Chromatography

HPLC is a powerful analytical technique used to separate, identify, and quantify individual components in a complex mixture. In HPLC, a sample containing the target substance is dissolved in a solvent and injected into a column packed with a stationary phase, in this case L1 which is defined by USP as octadecyl silane (ODS or C18) chemically bonded to porous silica or ceramic particles.

The column is then flushed with a mobile phase, in this case a water-acetonitrile solution that carries the sample components through the stationary phase at different rates. The individual components in the mixture (solution with sample particulates) will interact with the stationary phase to varying degrees, resulting in different retention times.

As the components exit the column, they are detected by a detector, which generates a signal proportional to the concentration of each component. The most common type of detector used in HPLC is the UV detector, which measures the absorption of UV light by the components as they pass through the detector.

By comparing the retention times and detector signals of the target substance with those of known standards, the concentration of the target substance in the sample can be determined by measuring the area under the peaks. i.e., If we know the retention time for T3 when moved through the column by a water-acetonitrile solution through L1 stationary phase (9.9 minutes to 10.9 minutes in our setup), then we can plot an intensity vs time graph and identify the T3 peak at the known retention time and calculate the area under the peak to measure absorption of the sample at that time. We can then compare that absorption to the known T3 in the reference standard and the average absorption measured in the reference standard to determine the T3 concentration in the sample using the equation:

$$T_{sample} = \frac{W_{Tstd}}{W_{sample}} \times \frac{A_{Tsample}}{A_{Tstd}}$$

Where W_{Tstd} is the weight of T3 or T4 in the standard injection solution (mg), $A_{Tsample}$ is the area under the T3 or T4 peak of the sample injection (mAU), A_{Tstd} is the area under the T3 or

T4 peak of the reference standard injection (mAU), W_{sample} is the total weight of the sample (mg), T_{sample} is the weight of T3 or T4 in the sample on an "As is basis" (µg/mg).

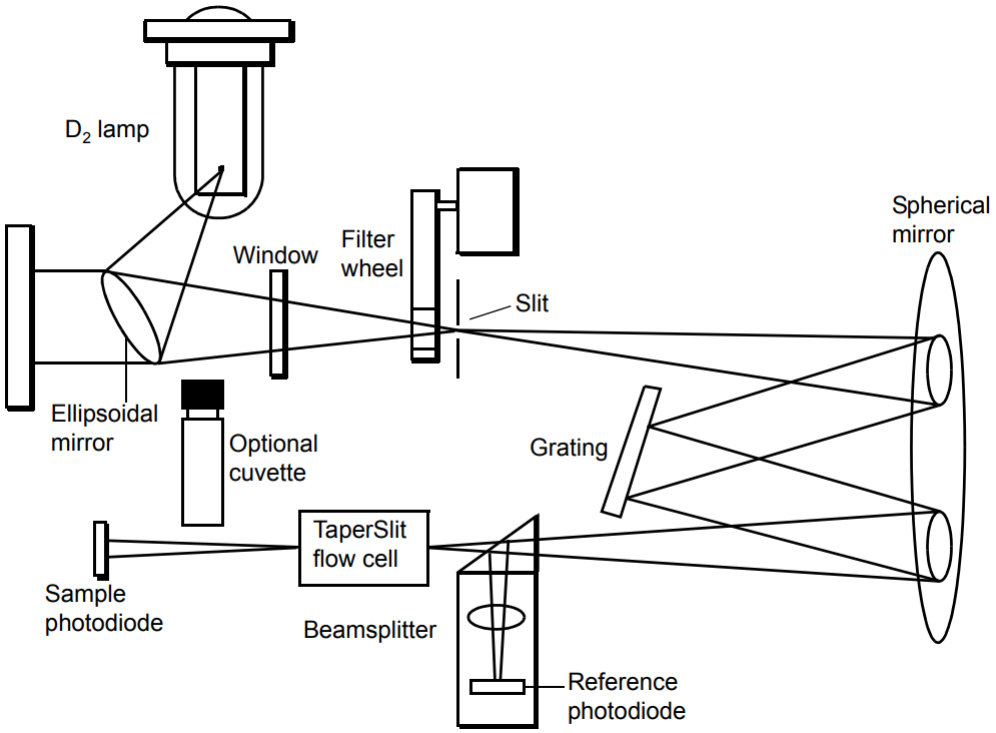

Figure 2 HPLC UV/Visible detector optics assembly.

The detector in Figure 2 provides an efficient design for high light throughput. The ellipsoidal mirror collects light from the lamp and focuses it through the filter wheel onto the entrance slit. The spherical mirror directs light toward the grating. A different portion of the spherical mirror focuses dispersed light of a particular wavelength band, determined by the grating angle, onto the entrance of the flow cell. Light exiting the flow cell passes through the cuvette location to the sample photodiode. The beam splitter, located just ahead of the flow cell, diverts a portion of the light to a reference photodiode. When you enter a new wavelength through the detector's front panel, the detector rotates the grating to the appropriate position. The preamplifier board integrates and digitizes the currents from the photodiodes for processing by the signal processing electronics and output to a computer, chart recorder, or integrator.

The TaperSlit flow cell used in this detector renders the detector baseline less sensitive to changes in mobile phase refractive index (RI). RI changes occur during gradient separations or result from temperature or pump-induced pressure fluctuations. To achieve RI immunity, a combination of a spherical mirror, a lens at the entrance of the flow cell, and a taper to the internal bore of the flow cell prevents light rays from striking the internal walls of the flow cell. An additional feature of the TaperSlit flow cell and the reason for its name is the shape of the flow cell entrance, which matches the shape of the entrance slit. The detector achieves higher light throughput for a given spectral resolution via the TaperSlit cell design, compared to a conventional flow cell with a circular entrance. As shown in Figure 3, in a conventional cell, light bends and hits the wall of the flow cell. Four beams go in, but only two come out. In the TaperSlit analytical cell, the combination of the lens and TaperSlit bore geometry prevents light from hitting the cell walls. Four beams go in, and four beams come out. The standard analytical, inert, and LC/MS cells have a path length of 10 mm.

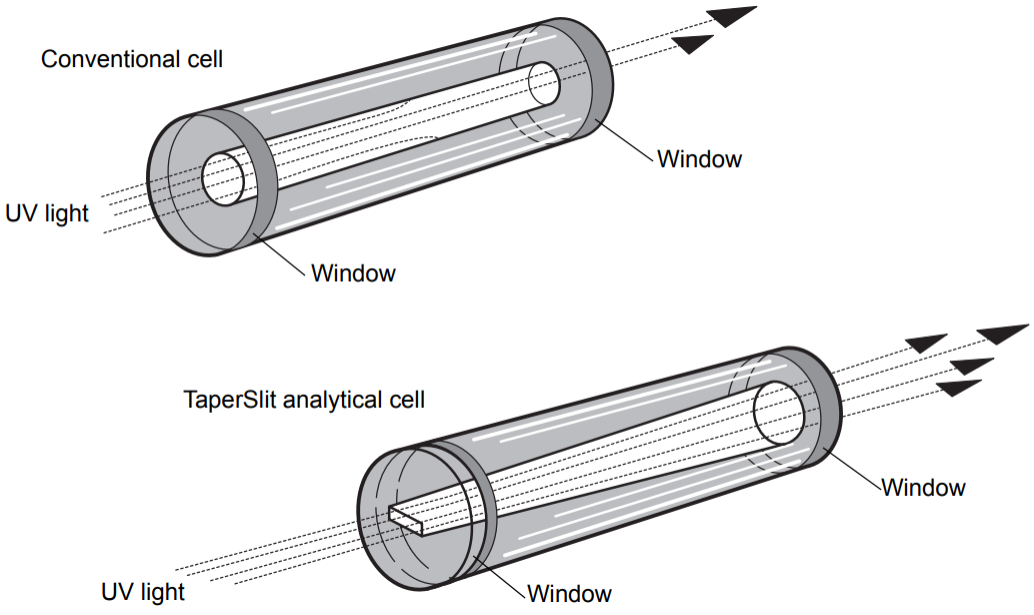

Figure 3 Comparison of flow cell characteristics.

The detector provides a Hamming filter to minimize noise. The Hamming filter is a digital finite impulse response filter, which creates peak height degradation and enhances the filtering of high frequency noise. The behavior of the filter depends on the filter time-constant selected. The filter time-constant adjusts the filter response time to achieve an optimal signal-to-noise ratio.

The detector's deuterium arc lamp and integral erbium filter exhibit peaks in the transmission spectrum at known wavelengths. Upon startup, the detector verifies calibration by comparing the locations of these peaks with expected wavelengths based on calibration data stored in the detector's memory. If the results of this verification differ from the stored calibration by more than 1.0 nm, the detector displays a failure message. The detector verifies, rather than recalibrates, on startup to avoid errors arising from residual materials left in the flow cell and/or the cuvette. The detector wavelength verification procedures establish an approximate "home" position using a grating homing sensor. Once "home" is established, the detector locates and references the 656.1 nm peak in the deuterium lamp emission spectrum.

The integral erbium filter moves into the common light path ahead of the flow cell entrance slit, enabling the detector to locate three additional spectral features at these wavelengths: 256.7 nm, 379.0 nm, 521.5 nm.

A frequently used mobile phase in HPLC is a 70:30 blend of acetonitrile and water. This mixture exhibits relatively low absorbance levels for wavelengths below 250 nm. T3 and T4 absorb light when the π electrons in their aromatic rings undergo a π-π^* transition, entering an excited state when the electrons move from the highest occupied molecular orbital to the lowest unoccupied molecular orbital by absorbing light of a particular wavelength. The energy required for this transition is defined by the equation:

$$E = \frac{hc}{\lambda}$$

Where E is the energy, h is Planck's constant, c is the speed of light, and λ is the light's wavelength. For T3 and T4 in the presence of this mobile phase, the wavelength of light absorbed for this transition is in the 220 nm to 240 nm range. Therefore, a wavelength of 230 nm is selected for the detector to maximize detection of T3 and T4 analytes and minimize any potential interference from the mobile phase. [6]

Pearson Correlation

The relationship between two sets of data may be quantified with a correlation value:

$$Corr_{X,Y} = \rho = \frac{\sum_{i=1}^{N}(X_i - \bar{X})(Y_i - \bar{Y})}{(N-1)s_X s_Y}$$

Where $Corr_{X,Y}$ is the correlation value between X and Y, $\overline{X}$ is the sample mean of X, $\overline{Y}$ is the sample mean of Y, N is the number of rows with no missing data for the pair of variables, s_X is the sample standard deviation of X, and s_Y is the sample standard deviation of Y.

A correlation value closer to 1 (or -1) shows a high correlation between data set X and data set Y. A correlation value closer to 0 shows a low correlation between data set X and data set Y. The confidence in this relationship can be quantified with a p-value. The p-value represents the chance that random data could produce a similarly strong relationship, or stronger. For a p-value $< \alpha$, we can be confident in the data. Generally, an α value of 0.05 is used.

Pearson's correlation confidence intervals are defined as:

$$\rho_L = \frac{e^{2Z_L} - 1}{e^{2Z_L} + 1}$$

$$\rho_U = \frac{e^{2Z_U} - 1}{e^{2Z_U} + 1}$$

where Z_L and Z_U are defined as:

$$Z_L = \frac{\ln(1+r) - \ln(1-r)}{2} - \frac{Z_{\alpha/2}}{\sqrt{N-3}}$$

$$Z_U = \frac{\ln(1+r) - \ln(1-r)}{2} + \frac{Z_{\alpha/2}}{\sqrt{N-3}}$$

where *r* is the Pearson sample correlation estimate of the unknown correlation, ρ.

To determine p-value, the hypotheses for a test that the correlation is 0 are as follows:

$H_0: \rho = 0$ versus $H_1: \rho \neq 0$. The test statistics for Pearson's correlation coefficient is:

$$t = \frac{r\sqrt{N-2}}{\sqrt{1-r^2}}$$

The p-value is then determined from the equation:

$$p = 2 \times P(T > t)$$

where T follows a t distribution with $N - 2$ degrees of freedom.

Correlation coefficients can be high or low (magnitude), and positive or negative (direction). Correlation coefficients vary from -1 to +1: whereas -1 and +1 indicate perfect negative and perfect positive correlation coefficients respectively, a correlation coefficient of 0 implies no correlation (zero relationship). Further, correlation coefficients lower than ± 0.40 (whether negative or positive 0.40) are said to be low, between ± 0.40 and ± 0.60 are moderate, and above ± 0.60 are high [7].

Thyroid Hormones

T3 and T4 hormones are essential for regulating metabolism in the body, including the rate at which cells use energy and produce heat. Imbalances in these hormones can lead to a wide range of health problems, including weight changes, fatigue, and changes in heart rate and body temperature. Therefore, thyroid hormones play an important role in an active pharmaceutical ingredient which, in tablet form, is used to treat patients with hypothyroidism.

Desiccated thyroid extract is a porcine thyroid gland which has been dried and powdered for medical use. Its first medical use was described in the late 19th century and by 1927 it had been synthesized by British chemists Charles Robert Harington and George Barger. Since the 1960s, use of desiccated thyroid extract has decreased in favor of the synthetic thyroxine, levothyroxine. Levothyroxine contains only T4 and is therefore largely ineffective for patients unable to convert T4 to T3 [8]. Those patients may choose to take the naturally derived desiccated thyroid extract which, in 2023 is the 117th most commonly prescribed medication in the United States with more than 5 million annual prescriptions [9].

Iodine accounts for 65% of the molecular weight of T4 and 59% of T3. If T3 and T4 were the only substances with iodine in a sample, we would then expect that a sample with 1,000 ppm and a process yield of 20% would have a T3 and T4 result of 1.69 µg/mg and 6.15 µg/mg, roughly 3.2× larger than is usually detected. This discrepancy has been described by experiments confirming that not all of the iodine content of thyroid extract is in the form of effective T3 and T4 and that actual content of available preparations varied more than the permitted 15% [10] [11] [12] [13].

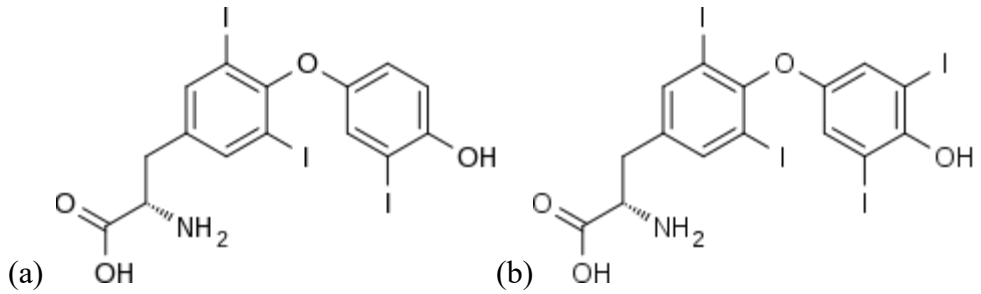

Figure 4 (a) Structure of (S)-triiodothyronine T3. (b) Structure of (S)-thyroxine T4.

Equipment

The XRF analyzer is an Olympus Vanta M Series 4-watt X-ray tube with 50 kV tungsten (W) anode and a large-area silicon drift detector which is designed to perform identification and analysis of elements contained within test samples from magnesium to uranium.

An HPLC system with an ultraviolet (UV) and visible range detector is used with a USP L1 column and separation module. The column is a Kinetex C18, 5µm, 250mm × 4.6mm, 100Å column from Phenomenex catalog number 00G-4601-E0.

Additional equipment for the HPLC testing include an analytical balance with a minimum of 0.01mg sensitivity, a pH meter, a bench top centrifuge, a vortex mixer, magnetic stir bars, sonicating bath, timer, temperature-controlled water bath, thermometer, repeat pipettors, volumetric glass pipettes, graduated cylinders, red iodine volumetric flasks, volumetric flasks, beakers, glass storage bottles, 16mm × 125mm glass screw top culture tubes with caps, 30mL syringe barrels, 2mL Amber HPLC vials, HPLC vial caps with TFE/SIL/TFE septa, 0.45µm PVDF filters, and weigh boats.

Additional materials used include USP reference standards (RS) for T3 and T4, Acetonitrile, Phosphoric Acid 85%, Sodium Chloride, Trishydroxymethylaminomethane (TRIS), Methimazole, 1:1 Hydrochloric Acid 50%, Ammonium Hydroxide, Pronase Protease, purified water, and thyroid powder test samples.

Experiment

Experimental Procedure

The XRF analyzer is powered on and calibration is verified by measuring a check standard.

Raw thyroid gland lots are received in lots with uniform-sized intra-lot boxes. $\sqrt{N} + 1$ boxes from each lot are sampled at five points each with the XRF analyzer as shown in Figure 5.

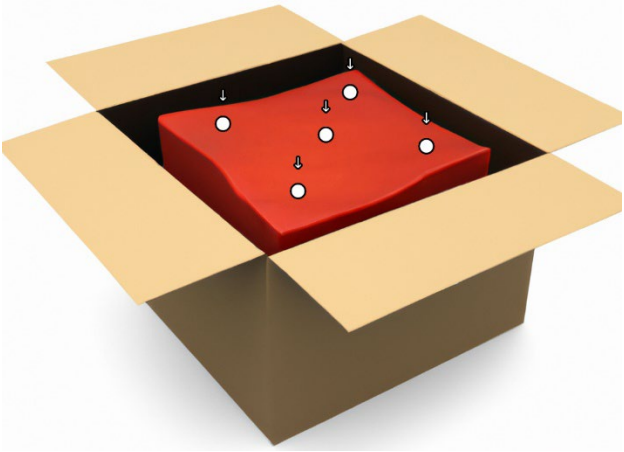

Figure 5 Visual guide of sample points for a box in an X pattern.

At the start of processing, a new batch number is assigned with material from one or more lots allocated to that batch. If one receiving lot is assigned to a batch, then that lot's XRF result is listed for that batch. If more than one receiving lot is assigned to a batch, then the weighted average of the lots' XRF results is listed for that batch.

The batch is then processed from raw thyroid glands into a fine powder.

At the end of processing, a sample of the fine powder is tested for T3 and T4 concentration via HPLC. The analysis of T3 and T4 samples begins with a protease hydrolysis to release the T3 and T4 from the powder. Comparison of the free T3 and T4 to the equivalent USP reference standards by HPLC reversed phase chromatography is then used to determine the content of T3 and T4 in the powder samples.

One liter of reducing buffer solution is prepared with 6.43g ± 0.1g sodium chloride, 4.85g ± 0.1g TRIS base, 5.71g ± 0.1g methimazole, and approximately 800 ml of purified water in an Erlenmeyer flask. The pH of the solution is adjusted to 8.4 ± 0.05 by adding 1:1 hydrochloric acid. The solution is then transferred to a 1L volumetric flask, capped, inverted several times to mix, transferred to a 1L Erlenmeyer flask and covered. Samples are prepared in triplicate and the average result is reported for each batch (4 significant figures). The sample is weighed at full strength (4X USP, 152µg of T4 per 65mg of powder) which is 16mg ± 2mg of powder per tube. A control sample is tested in triplicate in each HPLC run with the three control samples spaced evenly throughout the run.

A proteolytic enzyme solution is prepared by mixing (N+1)×15.75mg ± 5mg of pronase with (N+1)×5.25mL of the reducing buffer solution in an Erlenmeyer flask for 10 minutes, where N is the number of tubes in the run. 5ml of proteolytic enzyme solution is added to each sample and control tube. Each tube is vortexed for a minimum of 3 seconds and placed into a water bath at 37°C ± 1°C where they are digested for 28 hours ± 29 minutes with a cover protecting the samples from light exposure. Each tube is vortexed 3 more times throughout the digestion process to ensure effective dispersion.

The purity factors labeled for the T3 and T4 USP reference standards (RS) are adjusted based on results from the sample's loss on drying tests (4 significant figures) to weigh the appropriate amount of USP RS for each batch. The adjusted purity factor is then used with the USP T3 and T4 RS weights (22.50mg ± 2mg and 95.00mg ± 9mg, respectively) and divided by 2.5 to account for the volume of the 250mL volumetric flask used in the stock standard solution. The stock standard solution is prepared by mixing 70mL Acetonitrile, 70 mL purified water, and 0.125mL NH_4OH in a 250mL volumetric flask with the adjusted weights for T3 and T4 USP reference

standards and agitated until dissolved. Then Q.S. with a 1:1 Acetonitrile/Purified Water solution then capped and inverted until mixed. An intermediate standard solution is prepared by adding 5mL of the stock standard solution to a 250mL volumetric flask Q.S. to 250mL with reducing buffer solution, then capped and inverted until mixed. A working standard solution is prepared by adding 10mL of the intermediate standard solution into a culture tube with 4mL of Enzyme Deactivating Solution then capped and agitated for 10 seconds. The tube is then used to fill 6 amber HPLC vials with 1.5mL to 2 mL of the Working Standard solution. Mobile phase is prepared through HPLC system mixing with the thyroid mobile phase A:B solution based on the qualified column and the HPLC system being used. For the devices used in this experiment, this includes using a 1L volumetric flask filled approximately halfway with purified water with 5mL phosphoric acid added and Q.S. to 1L with purified water for mobile phase A. Mobile phase B uses a 1L volumetric flask filled approximately halfway with Acetonitrile with 5mL phosphoric acid added and Q.S. to 1L with purified water. The ratio of mobile phase A to mobile phase B used as the mobile phase solution is 7:3.

An enzymatic deactivation solution is prepared in a 100mL volumetric flask using 30mL of Acetonitrile with 1mL of phosphoric acid, then Q.S. to 100mL with Acetonitrile and inverting to mix. The sample tubes are removed from the water bath and 2ml of an enzymatic deactivation solution is pipetted into each tube. The tubes are vortexed and centrifuged at 2,000rpm ± 200rpm for 5 minutes. The samples are then filtered with a 0.45um filter with a 32mm diameter by pouring the supernatant fluid into the barrel of the corresponding syringe/filter. 1.5mL to 2mL of the supernatant is collected in the corresponding HPLC vial for each sample.

The HPLC is set up with a 230nm detector with injection volume set to deliver 100µL for a run time of 30 minutes ± 7 minutes at a flow rate of 1.0mL/min ± 0.5mL/min. The vials are placed in

the corresponding sample/control/standard positions on the HPLC automatic injector tray. A pronase blank is analyzed first to ensure that there are no atypical peaks eluting that could interfere with the control or sample injections and then 1 injection of the working standard and 1 injection of a previously used control are used to observe peak separation before running the rest of the samples.

Using the USP reference standards (RS) and purity factor adjustments, USP RS dry weight is calculated by the formula:

$$W_{USP,RS} = W_{RS} \times P_{RS}(1 - LOD\%_{RS})$$

Where $W_{USP,RS}$ is the USP RS dry weight, W_{RS} is weight of the reference standard, P_{RS} is the purity factor for the reference standard, and $LOD\%_{RS}$ is the loss on drying result.

The coefficient of variation C_v is calculated as:

$$C_v = \frac{\sigma}{\mu} = \frac{\sqrt{\frac{\sum(X - \bar{X})}{n - 1}}}{\bar{X}} \times 100$$

Where σ is the standard deviation, μ is the mean, X is the peak area, n is the number of results, and $\bar{X}$ is the average peak area.

Measurement Uncertainties

Iodine detected through X-ray fluorescence on raw product is only the iodine levels detected at the top surface of sample boxes, shown in Figure 5. Box weights range from 10lbs to 60lbs, filled with thyroid glands. The weights for porcine thyroid glands measured from 81 boxes is 7g to 23g. Therefore, each box may be filled with 200 to 4,000 thyroid glands. Given that suppliers advertise a capacity of 200 to 2,000 slaughters per day, it is reasonable to expect that these boxes are filled over the course of the workday before being frozen and sold.

This leaves several hours for blood to accumulate at the bottom of the plastic-lined box and the weight of glands in the middle and top of the box to exert pressure on the glands at the bottom of the box. Experiments have shown that while blood around the thyroid gland at slaughter may have typical hormone levels for the circulatory system, the blood within the thyroid gland has a very high concentration of thyroid hormones. Pressure exerted on the glands at the bottom of the box causes some of the high hormone concentrated blood to squeeze out. These two factors show that there may be a difference in iodine concentration at the top, middle, and bottom of the sample so iodine detected at the top surface may not be representative of the sample.

In XRF testing, Tungsten produces a broader spectral peak than rhodium, which can result in lower spectral resolution and reduced accuracy in some applications. The higher X-ray intensity produced by tungsten can lead to greater background noise in the analysis, which can affect the detection limits and accuracy of the instrument.

Using a handheld XRF device which takes 2 to 3 minutes to report an accurate result to measure iodine concentration leaves room for operator error by shifting while holding the device, causing an inconsistent test area across the sample. For a non-homogeneous sample and operator fatigue throughout the testing process, this may cause inconsistent results as the detector shifts from areas with more or less blood at the surface and the distance from the detector from the sample shifts more throughout testing.

In HPLC testing, the Graphitized Carbon Black (GCB) C18 stationary phase has been known to bind long chain per- and polyfluoroalkyl substances (PFAS). Some problems can occur where low recoveries are achieved due to irreversible binding of certain PFAS compounds, most likely the longer chain PFAs. PFAS may be introduced to the product from contact with plastic lining

before and during processing. PFAS may be introduced to the sample from pipette tips and filters.

Results

A total of 62 samples were processed and measured using the established experimental procedure described above. Figure 6 shows the results obtained for both T3 and T4 hormones as correlation plots of Iodine concentration (ppm) vs hormone concentration (µg/mg). Figure 6,a is the correlation plot for T3 hormone and Figure 6,b is the correlation plot for T4 hormone. For both hormones, Pearson correlation values of 0.441 and 0.447 were achieved for iodine concentration vs T3 and T4 concentration, as indicated by Figure 6,a and 6,b respectively, (for n = 62 and a confidence interval of 95%,). These results suggest a moderate correlation between iodine concentration in raw thyroid glands to thyroid hormone concentration in post-processed thyroid powder.

(a)

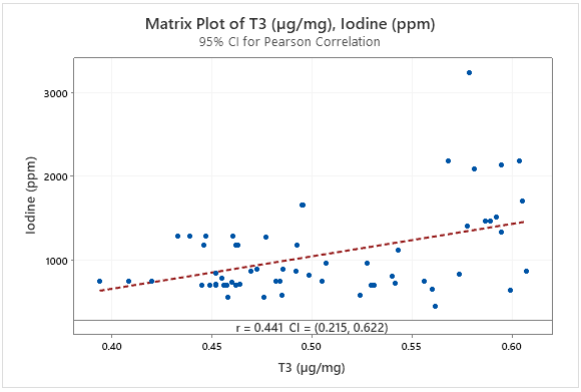

(b)

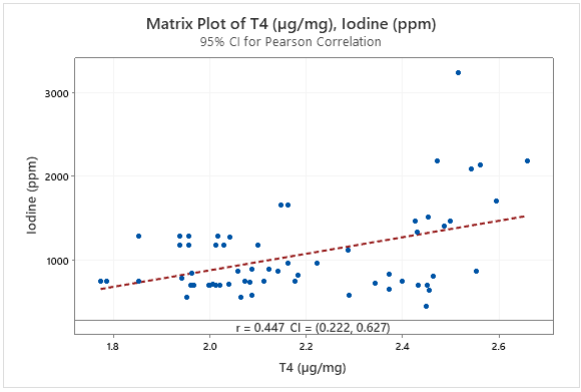

Figure 6 (a) Plot of iodine (ppm) vs dry basis T3 (µg/mg). (b) Plot of iodine (ppm) vs dry basis T4 (µg/mg).

The T3 and T4 values are dry basis, a calculated value based on the "as is" results and moisture content measured from loss on drying (LOD) testing. The "as is" results come directly from HPLC testing and show the true concentration of the hormones in the sample. This value is adjusted to dry basis to standardize the measurements by removing volatile components such as

moisture content. i.e., To compare results between batches, the efficacy of the drying process should not be a factor, so dry basis results remove the variability of the drying process with the equation:

$$T3_{Dry\ basis} = \frac{T3_{As\ is}}{1 - LOD\%}$$

Due to some batches including material from multiple lots of raw material, the iodine concentration values listed for each batch are the weighted average of iodine concentration detected in the batch's input lots.

Next, I have tested the samples received in batches from supplier A. Figure 7 shows a time-ordered plot of the iodine concentration detected in the received batches. The pack date is the average pack date of the boxes sampled in the respective lots. An apparent drop can be easily identified from Figure 7 occurring between late 2017 to early 2018. This drop helped identify a shift in quality of raw material from the supplier several months before HPLC testing from post-processed material would have indicated a shift. The results provide evidence that measuring iodine can serve as predictor of raw material quality.

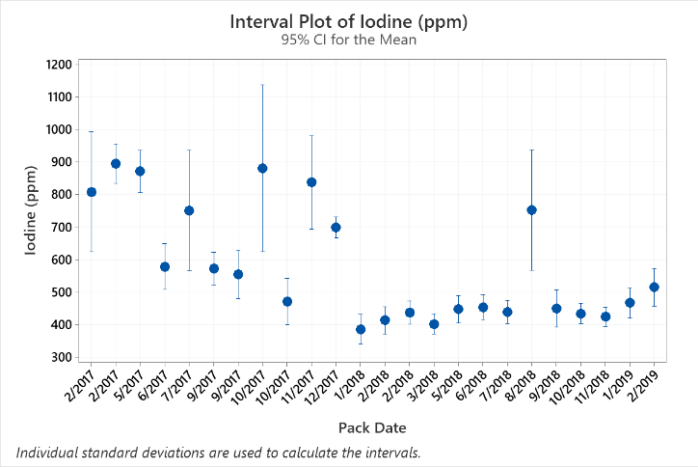

Figure 7 Plot of iodine (ppm) vs pack date for batches from supplier A.

Discussion

Our research question was as follows: what is the relationship between iodine concentration in raw thyroid glands and thyroid hormone concentration in fine milled thyroid powder? We have found that there is a moderate relationship between iodine concentration in raw samples and thyroid hormones in fine milled thyroid powder.

With this information, our team is able to prioritize lots with higher or lower iodine concentrations to better forecast our post-process inventory months in advance. The established correlation also helps to plan product blending and sales several months ahead of time while, through continuous process improvement metrics, establishing process control and significantly reducing variability in our end product. This builds trust in our product, our process, and our team.

We are also able to use supplier-specific average iodine concentrations to identify any out-of-control trends in raw material from suppliers to adjust allocation rates months before HPLC testing on post-processed thyroid would alert our team to changes to our supplier's material. Generating a time ordered control chart for suppliers can also help us identify a date range when our supplier may have shifted their process to help our team and our suppliers better understand which process shifts may have positive or negative impacts on raw thyroids.

Limitations in defining a strong relationship between iodine concentration and thyroid hormone concentration include: (1) a significant portion of iodine content in the samples are not in the form of effective T3 and T4; (2) XRF testing performed at the top surface of a non-homogeneous sample is not a perfect representative of the sample; (3) extended hold periods of intermediate material have shown a decrease in T4 and increase in T3 in the material which would not affect iodine concentration of raw material, but would affect thyroid hormone concentration in post-

processed material; (4) small-scale suppliers have a wider slaughter date range which may increase intra-batch variability.

Summary

In summary, a moderate correlation between iodine concentration and thyroid hormone concentration was identified by testing with X-ray fluorescence on raw products and high-performance liquid chromatography on finished product. This correlation helps to monitor raw product trends and to confidently schedule operations, sales, and procurement plans several months earlier than would otherwise be possible.

Metrics established from iodine concentration measurements help our team establish process control and learn with our suppliers about impacts to raw product.

Tables

Table 1, data used for Figure 6:

Batch	Lot	Dry Basis T3 (µg/mg)	Dry Basis T4 (µg/mg)	Weighted Average: Iodine (ppm)
TSE-001	001	0.592	2.454	1517.1
TSE-002	002	0.460	2.083	737.2
TSE-003	003	0.495	2.148	1663.2
TSE-004	004	0.498	2.183	826.9
TSE-005	005	0.462	2.020	699.3
TSE-006	005	0.456	1.998	699.3
TSE-007	005	0.457	2.012	699.3
TSE-008	005	0.452	1.961	699.3
TSE-009	005	0.449	2.000	699.3
TSE-010	006	0.492	2.101	1175.5
TSE-011	005	0.445	1.967	699.3
TSE-012	006	0.462	2.029	1175.5
TSE-013	007	0.394	1.773	753.4
TSE-014	007	0.408	1.785	753.4
TSE-015	006	0.446	1.938	1175.5
TSE-016	005	0.452	2.007	714.0

Batch	Lot	Dry Basis T3 (µg/mg)	Dry Basis T4 (µg/mg)	Weighted Average: Iodine (ppm)
TSE-017	006	0.463	2.013	1175.5
TSE-018	007	0.420	1.853	745.6
TSE-019	006	0.446	1.955	1175.5
TSE-020	003	0.495	2.162	1663.2
TSE-021	008	0.464	2.039	716.8
TSE-022	004	0.455	1.943	785.5
TSE-023	009	0.439	1.938	1287.6
TSE-024	009	0.460	1.956	1287.6
TSE-025	009	0.447	2.018	1287.6
TSE-026	007	0.452	1.962	847.5
TSE-027	009	0.433	1.852	1287.6
TSE-028	006	0.477	2.042	1276.7
TSE-029	010	0.505	2.176	751.4
TSE-030	010	0.482	2.112	751.4
TSE-031	010	0.484	2.072	751.4
TSE-032	011	0.579	2.516	3244.4
TSE-033	012	0.556	2.399	756.4
TSE-034	013	0.492	2.142	872.1
TSE-035	013	0.469	2.059	872.1
TSE-036	014	0.473	2.087	895.4
TSE-037	013	0.486	2.122	893.7
TSE-038	015	0.524	2.288	578.3
TSE-039	015	0.485	2.087	578.3
TSE-040	016	0.476	2.064	554.3
TSE-041	016	0.458	1.953	554.3
TSE-042	017	0.594	2.561	2141.7
TSE-043	018	0.577	2.486	1404.3
TSE-044	019	0.581	2.542	2093.4
TSE-045	020	0.603	2.659	2180.6
TSE-046	021	0.589	2.425	1472.0
TSE-047	021	0.586	2.498	1464.7
TSE-048	022	0.595	2.431	1332.8
TSE-049	023	0.607	2.552	874.5
TSE-050	024	0.599	2.455	646.8
TSE-051	019	0.605	2.594	1712.8
TSE-052	020	0.568	2.472	2180.6
TSE-053	025	0.560	2.372	660.2
TSE-054	026	0.527	2.222	967.2
TSE-055	026	0.507	2.163	967.2

Batch	Lot	Dry Basis T3 (µg/mg)	Dry Basis T4 (µg/mg)	Weighted Average: Iodine (ppm)
TSE-056	027	0.543	2.287	1127.4
TSE-057	028	0.542	2.342	725.2
TSE-058	024	0.562	2.449	450.1
TSE-059	029	0.531	2.451	707.7
TSE-060	029	0.530	2.431	707.7
TSE-061	030	0.540	2.464	812.9
TSE-062	031	0.574	2.373	839.9

Table 2, data used for Figure 7:

Lot	Average: Iodine (ppm)	Pack Date
005	699.3	12/21/2017
007	753.4	08/13/2018
032	881.2	10/13/2017
010	751.4	07/22/2017
033	808.3	02/10/2017
034	837.6	11/15/2017
013	872.1	05/10/2017
014	895.4	02/17/2017
015	578.3	06/26/2017
016	554.3	09/29/2017
035	571.5	09/11/2017
036	467.3	01/13/2019
037	514.9	02/06/2019
038	452.9	06/11/2018
039	385.6	01/17/2018
040	446.6	05/29/2018
041	470.2	10/30/2017
042	401.8	03/30/2018
043	436.7	02/23/2018
044	449.8	09/20/2018
045	439.0	07/26/2018
046	412.7	02/08/2018
047	423.6	11/14/2018
048	433.9	10/20/2018

References

[1] W. Boron *Medical Physiology (3rd ed.)* (Elsevier, 2016) **Chapter 49**. ISBN 9781455743773.

[2] Jerrold T. Bushberg, John M. Boone. *The Essential Physics of Medical Imaging* (2011) ISBN: 9780781780575.

[3] Vanta Family X-Ray Fluorescence Analyzer manual.

[4] Allisy-Roberts P, Williams J. Farr's *Physics for Medical Imaging*. W.B. Saunders Company. (2007) ISBN:0702028444.

[5] X-Ray Data Booklet Table 1-2. Lawrence Berkeley National Laboratory https://xdb.lbl.gov/Section1/Table_1-2.pdf

[6] Willard, H. H. and others. *Instrumental Methods of Analysis*, 6th ed. Litton Educational Publishing, Inc., 1981.

[7] Obilor, Esezi Isaac & Amadi, Eric. (2018). Test for Significance of Pearson's Correlation Coefficient.

[8] Wiersinga, W.M. (2002). Thyroid Hormone Replacement Therapy. *Hormone Research in Paediatrics*, 56, 74 - 81.

[9] https://clincalc.com/DrugStats/Drugs/Thyroid *ClinCalc.* Retrieved 25 April 2023.

[10] MACGREGOR AG. Why does anybody use thyroid B.P.? Lancet. 1961 Feb 11;1(7172):329-32. doi: 10.1016/s0140-6736(61)91498-2. PMID: 13764789.

[11] CATZ B, GINSBURG E, SALENGER S. Clinically inactive thyroid U.S.P. A preliminary report. N Engl J Med. 1962 Jan 18;266:136-7. doi: 10.1056/NEJM196201182660308. PMID: 13877407.

[12] VINCENT J. PILEGGI, ORVILLE J. GOLUB, NORMAN D. LEE, Determination of Thyroxine and Triiodothyronine in Commercial Preparations of Desiccated Thyroid and Thyroid Extract, The Journal of Clinical Endocrinology & Metabolism, Volume 25, Issue 7, 1 July 1965, Pages 949–956, https://doi.org/10.1210/jcem-25-7-949

[13] C. N. MANGIERI, M. H. LUND, Potency of United States Pharmacopeia Desiccated Thyroid Tablets as Determined by the Antigoitrogenic Assay in Rats, The Journal of Clinical Endocrinology & Metabolism, Volume 30, Issue 1, 1 January 1970, Pages 102–104, https://doi.org/10.1210/jcem-30-1-102